Published in final edited form as:
Exp Lung Res. 2011 August ; 37(6): 327–343. doi:10.3109/01902148.2011.566673.

Diverse injurious stimuli reduce protein tyrosine phosphatase-μ expression and enhance epidermal growth factor receptor signaling in human airway epithelia

Sang W. Hyun[1], **Ian E. Anglin**[1], **Anguo Liu**[1], **Shiqi Yang**[1], **John D. Sorkin**[2], **Erik Lillehoj**[3], **Nicholas K. Tonks**[4], **Antonino Passaniti**[5], and **Simeon E. Goldblum**[6]

[1]Department of Medicine, Mucosal Biology Research Center, University of Maryland, Baltimore, Maryland, USA

[2]VA Maryland Health Care System, Geriatric Research, Education, and Clinical Center, Baltimore, Maryland, USA

[3]Department of Pediatrics, University of Maryland, Baltimore, Maryland, USA

[4]Cold Spring Harbor Laboratory, Cold Spring Harbor, New York, USA

[5]Department of Pathology and the Marlene and Stewart Greenebaum Cancer Center, University of Maryland School of Medicine, Baltimore, Maryland, USA

[6]Department of Medicine, Mucosal Biology Research Center, University of Maryland, Baltimore, Maryland, USA; and Department of Pathology and the Marlene and Stewart Greenebaum Cancer Center, University of Maryland School of Medicine, Baltimore, Maryland, USA

Abstract

In response to injury, airway epithelia utilize an epidermal growth factor (EGF) receptor (EGFR) signaling program to institute repair and restitution. Protein tyrosine phosphatases (PTPs) counterregulate EGFR autophosphorylation and downstream signaling. PTPμ is highly expressed in lung epithelia and can be localized to intercellular junctions where its ectodomain homophilically interacts with PTPμ ectodomain expressed on neighboring cells. We asked whether PTPμ expression might be altered in response to epithelial injury and whether altered PTPμ expression might influence EGFR signaling. In A549 cells, diverse injurious stimuli dramatically reduced PTPμ protein expression. Under basal conditions, small interfering RNA (siRNA)-induced silencing of PTPμ increased EGFR Y992 and Y1068 phosphorylation. In the presence of EGF, PTPμ knockdown increased EGFR Y845, Y992, Y1045, Y1068, Y1086, and Y1173 but not Y1148 phosphorylation. Reduced PTPμ expression increased EGF-stimulated phosphorylation of Y992, a docking site for phospholipase C (PLC)γ1, activation of PLCγ1 itself, and increased cell migration in both wounding and chemotaxis assays. In contrast, overexpression of PTPμ decreased EGF-stimulated EGFR Y992 and Y1068 phosphorylation. Therefore, airway epithelial injury profoundly reduces PTPμ expression, and PTPμ depletion selectively increases phosphorylation of specific EGFR tyrosine residues, PLCγ1 activation, and cell migration, providing a novel mechanism through which epithelial integrity may be restored.

Address correspondence to Simeon E. Goldblum, MD, The Mucosal Biology Research Center, University of Maryland Baltimore, 20 Penn Street, HSFII, Room S303D, Baltimore, MD 21201, USA. sgoldblu@mbrc.umaryland.edu.

Declaration of interest: The authors report no conflicts of interest. The authors alone are responsible for the content and writing of the paper.

Keywords

epithelial cell migration; epithelial cell repair; epidermal growth factor receptor; protein tyrosine phosphatase-μ; protein tyrosine phosphorylation; phospholipase Cγ

The epithelial cells lining the airways provide a protective barrier against inhaled chemical irritants, allergens, and infectious agents [1]. The intact epithelium is maintained through tightly orchestrated cell proliferation, spreading, migration, and programmed cell death. In response to injury, the epithelium undergoes repair and restitution through mechanisms that center around cell migration [1–3]. These normally quiescent polarized cells form a tightly sealed surface through complex intercellular junctions including the tight junction (tj) or the zonula occludins and the adherens junction, or the zonula adherens (ZA) [4, 5]. For migration to occur, cells must first disengage from neighboring cells, in part, through disassembly of the ZA multiprotein complex [6].

Epidermal growth factor receptor (EGFR) activation and downstream signaling have been implicated in airway epithelial repair and restitution [2, 3, 5, 7]. EGFR expression in normal human airway epithelia is low [8, 9] but increases in response to diverse injurious stimuli [1]. Although EGFR activation can increase cell proliferation, differentiation, and survival [7], it accelerates epithelial wound healing through phospholipase C (PLC)γ-mediated cell migration [3, 7, 10, 11]. The mechanisms through which EGFR activation may promote cell migration include actin reorganization [12, 13], focal adhesion disassembly [11], and increased tyrosine phosphorylation of ZA proteins [14–16], which, through inside-out signaling, reduces homophilic adhesion between opposing E-cadherin ectodomains [17].

EGFR is a membrane-spanning receptor protein tyrosine kinase (PTK) that is comprised of an NH_2-terminal, ligand-binding ectodomain coupled to an intracellular catalytic domain and its tyrosine phosphorylation sites [18]. Ligand binding to the EGFR ectodomain induces receptor dimerization, intrinsic tyrosine kinase activity, and autophosphorylation of specific tyrosine residues, including Y845, Y992, Y1045, Y1068, Y1086, Y1148, and Y1173 [18]. Upon phosphorylation, these tyrosines serve as docking sites within the EGFR cytoplasmic domain for specific downstream signaling molecules containing src homology (SH)2 or phosphotyrosine-binding domains. Autophosphorylation of Y992 and Y1173 generates docking sites for PLCγ [18, 19], which contains 2 SH2 domains and 3 tyrosine phosphorylation sites, Y771, Y783, and Y1254, essential to its recruitment and activation [20, 21]. PLCγ_1 hydrolyzes phosphatidylinositol 4,5-biphosphate (PIP_2), producing inositol 1,4,5-triphosphate (IP_3) and diacyl-glycerol (DAG), which in turn, transiently increase intracellular Ca^{2+} and directly activate protein kinase C (PKC), respectively [20, 21]. PLCγ_1 recruitment to EGFR and its downstream signaling are required for EGFR-driven cell migration [10, 11].

In addition to its intrinsic kinase activity, activated EGFR also recruits nonreceptor PTKs, including src family and Jak-2 PTKs [18, 22], as well as protein tyrosine phosphatases (PTPs), including PTP1B, PTP_K, SHP-1, and SHP-2 [23–25]. These PTKs and PTPs phosphorylate/dephosphorylate distinct tyrosine residues within the EGFR COOH-terminus [25]. Interestingly, EGFR activation generates H_2O_2 [26], which can oxidize a crucial cysteine residue within the conserved catalytic domain of PTPs, attenuating PTP activity [27], further stabilizing and amplifying phosphotyrosine-dependent signaling. One PTP, PTPμ, is highly expressed in lung, including lung epithelia [28, 29]. This receptor PTP contains a putative ligand-binding ectodomain, a single transmembrane segment, and 2 intracellular catalytic domains, the second or COOH-terminus of which is inactive [29]. The extracellular domain of this ~200-kDa protein contains in tandem an NH_2-terminal MAM

(**M**eprins A and B, *Xenopus* **A**$_5$ glycoprotein, PTP**m**u) domain, an immunoglobulin (Ig)-like repeat, and 4 fibronectin (FN) III-like repeats [29, 30]. The MAM domain, the Ig repeat, and 1 or more of the FN III-like repeats form a structural unit that is essential and sufficient for homophilic adhesion [30–34]. In extracts of rat lung and various cell lines, PTPμ interacts with the classical cadherins, E-cadherin, N-cadherin, and cadherin-4 [35]. PTPμ also directly binds to the cytoplasmic domain of the least conserved classical cadherin, vascular endothelial-cadherin, and counterregulates its tyrosine phosphorylation state [36]. In these same studies, PTPμ was found to maintain barrier integrity in human lung microvascular endothelia. Whether PTPμ interacts with catenins is less clear [37]. PTPμ contains a target motif in its fourth FN III-like repeat, RPRRTKK, that is recognized and cleaved by subtilisin/kexin-like endoproteases [38]. Such proteolytic processing results in 2 ~100-kDa cleavage products, one of which contains almost the entire ectodomain. Whether these PTPμ fragments retain PTP or other signaling activity is unclear. Although the regulation of PTPμ expression and activity is not well understood, expression of full-length PTPμ and its proteolysis increase in cells as they achieve confluence and undergo contact inhibition [38]. In the current studies, we asked whether airway epithelial injury might reduce PTPμ expression, and whether manipulation of PTPμ expression might influence EGFR autophosphorylation and downstream signaling, thereby accelerating EGFR-driven epithelial repair.

MATERIALS AND METHODS

Cell culture

Human lung A549 cells are an alveolar type II cell line derived from a lung adenocarcinoma (American Type Culture Collection, Manassas, VA). 16HBE14o$^-$ and 1HAEo$^-$ are simian virus 40 (SV40) T antigen–transformed human bronchial and tracheal epithelial cell lines that were provided by Dr. Dieter Gruenert (California Pacific Medical Center Research Institute, San Francisco, CA). BEAS-2B is a SV40-transformed human bronchial epithelial cell line that was provided by Dr. Sekhar Reddy (Johns Hopkins University, Baltimore, MD). Cells were cultured in Dulbecco's modified Eagle's medium (DMEM) enriched with 10% fetal bovine serum (Hyclone Laboratories, Logan, UT), 5 mM L-glutamine, nonessential amino acids, and vitamins in the presence of penicillin (50 U/mL) and streptomycin (50 μg/mL) (Sigma). Primary human small airway epithelial cells (SAECs) (Lonza Walkersville, Walkersville, MD) were cultured in predefined small airway growth medium (Lonza) containing hydrocortisone, human EGF, epinephrine, transferrin, insulin, retinoic acid, triiodothyronine, and fatty acid–free bovine serum albumin (BSA). Only SAEC passages 2 to 4 were studied.

PTPμ and EGFR immunoblotting

Cells were thoroughly rinsed with ice-cold HEPES buffer, and solubilized with ice-cold lysis buffer containing 50 mM Tris-HC1 (pH 7.4), 1% Nonidet P-40, 0.25% sodium deoxycholate, 150 mM NaCl, 1 mM phenylmethylsulfonyl fluoride, 1 mg/mL leupeptin, 1 mg/mL pepstatin A, 1 mg/mL aprotinin, 1 mM vanadate, 1 mM sodium fluoride, 10 mM disodium pyrophosphate, 500 μM *p*-nitrophenol, and 1 mM phenylarsine oxide (PAO) (all purchased from Sigma) as described [36]. The cell lysates were assayed for protein concentration with a Bio-Rad DC Protein assay kit (Bio-Rad Laboratories, Hercules, CA). Equal amounts of protein were resolved by electrophoresis on 4–12% gradient sodium dodecyl sulfate (SDS)-polyacrylamide gels (Novex, San Diego, CA) and transferred to polyvinylidene fluoride (PVDF) membranes (Millipore, Bedford, MA). The blots were probed with a murine monoclonal antibody raised against the intracellular juxtamembranous segment of PTPμ (SK15; 1:500) (Santa Cruz Biotechnology, Santa Cruz, CA) followed by horseradish peroxidase (HRP)-conjugated goat anti-mouse immunoglobulin G (IgG) (United

Biotech, Mountain View, CA) in 5% milk, Tris-buffered saline Tween 20 (TBS-T) and developed with enhanced chemiluminescence (ECL) (GE Healthcare Amersham, Piscataway, NJ) [36]. In selected experiments, cell lysates were immunoblotted with murine anti-EGFR antibodies (BD Biosciences Pharmingen, San Jose, CA) followed by HRP-conjugated anti-mouse IgG. To confirm equivalent protein loading and transfer, blots were stripped with 100 mM 2-mercaptoethanol, 2% SDS, 62.5 mM Tris-HCI, pH 6.7, and reprobed with 0.5 ng/mL of murine anti-*Physarum* β-tubulin IgG2b (Boehringer-Mannheim, Indianapolis, IN) followed by HRP-conjugated anti-mouse IgG and again, developed with ECL. PTPμ immunoreactive bands and β-tubulin bands were each quantified by densitometry and PTPμ was normalized to β-tubulin.

Adenoviral infection and other injurious stimuli

Adenovirus (Ad) encoding for green fluorescent protein (Ad-GFP) were packaged and amplified in human embryonic kidney (HEK)293 cells. A549 cells cultured to confluence in 60-mm dishes were incubated for increasing times (1 to 6 days) with medium alone or packaged Ad-GFP (stock viral titer = 6.3×10^{10} plaque-forming units [PFU]) at a multiplicity of infection (MOI) of ~250. In other experiments, A549 cells were exposed to lipopolysaccharide (LPS) (100 μg/mL, 72 hours), tumor necrosis factor (TNFα) (200 ng/mL, 72 hours), H_2O_2 (5 mM, 48 hours), heat shock (43°C, 1 hour), hyperosmolarity (NaCl 200 mM, 24 hours), or medium alone. At each time point, the monolayers were lysed, and the lysates processed for PTPμ immunoblotting.

Knockdown of PTPμ and EGFR through siRNA technology

Small interfering RNA (siRNA) duplex products designed to target either PTPμ or EGFR as well as control siRNA duplexes that do not correspond to any known sequence in the human genome (Dharmacon, Lafayette, CO) were preincubated with Trans-Messenger transfection reagent (Qiagen, Valencia, CA) and the complexes presented to ~80% confluent A549 cells for 3 hours in the absence of serum as described [36]. At 72 hours, cells were lysed and processed for PTPμ or EGFR immunoblotting. To exclude off-target knockdown, cells transfected with PTPμ-targeting siRNAs were lysed and the lysates processed for immunoblotting with antibodies raised against 2 PTPs highly homologous to PTPμ, PTP (H-75; Santa Cruz Biotechnology) [39] and PTPλ (ab13223; Abcam) [40]. Once knockdown was established, the siRNAs were transfected into cells for studies of EGFR autophosphorylation, extracellular signal-regulated kinase 1/2 (ERK1/2) and PLCγ activation, and cell migration in wounding and chemotaxis assays as described below.

Ad-PTPμ infection to overexpress PTPμ

To regulate PTPμ expression in A549 cells, the AdEasy Vector System (Qbiogene, Carlsbad, CA) was used to generate a recombinant Ad encoding for wild-type PTPμ (Ad-PTPμ). A cDNA insert from a PTPμ plasmid that we have previously described [36] was released by Kpn 1 and Not 1 digestion and sub-cloned into a shuttle vector (pAdTrack-CMV; Qbiogene). The resultant shuttle plasmid was linearized through Pme 1 digestion and, with the Ad backbone plasmid (pAdEasy-1, Qbiogene), was used to transform electrocompetent *Esherichia coli* BJ5183. Recombinants were selected for kanamycin resistance and screened for recombination by Pac 1 restriction enzyme analysis for the appearance of 4.5-kb and 30-kb bands on agarose gel electrophoresis. The correct recombinant plasmids were used to transform in *E. coli* DH5α and bacterial lysates were passed through Maxiprep columns (Qiagen) for purification of Ad-PTPμ. Ad-PTPμ was linearized with Pac 1 digestion and transfected, in the presence of Ca_2PO_4, into HEK293 cells. After 7 to 10 days, cells were scraped off flasks with a rubber policeman, subjected to 3 freeze-thaw cycles, and virus harvested in the supernatants for presentation to fresh HEK293 cells and titration in a plaque-forming assay. A549 cells were transiently infected

with packaged Ad-PTPμ at MOIs of 5, 10, 50, 100, and 200, or an Ad-null vector control. At 48 hours, cells were lysed and the lysates processed for PTPμ, EGFR, phospho-EGFR, β-tubulin, and/or phospho-PLCγ immunoblotting. In other experiments, A549 cells transiently infected with either Ad-PTPμ or Ad-null were studied for cell migration in wounding and chemotaxis assays.

EGFR, PLCγ, and ERK activation

To delineate which specific tyrosines within the cytoplasmic domain of EGFR are counterregulated by PTPμ, lysates were processed for immunoblotting with a series of defined, epitope-mapped, rabbit polyclonal anti-phospho-EGFR antibodies that recognize Y845, Y992, Y1045, or Y1148 (Cell Signaling Technology, Danvers, MA), Y1086 (Zymed Labs, S. San Francisco, CA), or Y1173 (Cell Signaling Technology), all contained within the cytoplasmic domain of EGFR [18]. A murine monoclonal antibody was used to probe for phospho-EGFR Y1068 (Cell Signaling Technology). The blots were stripped and reprobed with anti-β-tubulin antibodies. For the PLCγ studies, the membranes were immunoblotted with rabbit anti-human phospho-PLCγ (Y783) antibody (Cell Signaling Technology) followed by goat anti-rabbit HRP-conjugated IgG (Pierce Chemicals) and developed with ECL [41]. To confirm equivalent protein loading and transfer, blots were stripped and reprobed for total PLCγ with rabbit anti-human PLCγ antibody (Cell Signaling Technology). For the ERK1/2 studies, the membranes were incubated with murine anti-human phospho-ERK1/2 antibodies (Sigma) followed by HRP-anti-murine IgG, and developed with ECL. To confirm equivalent protein loading and transfer, blots were stripped and reprobed with anti-ERK1/2 antibodies (Sigma).

PTPμ immunolocalization

A549 cells were seeded at 0.2×10^5 or 2×10^5 cells/well on coverslips in 6-well plates and cultured for 2 to 3 days to generate subconfluent and confluent monolayers, respectively. Cells were washed 3 times with phosphate-buffered saline (PBS) without Ca^{2+}/Mg^{2+}, fixed (3% paraformaldehyde at 37°C for 5 minutes), permeabilized (0.5% Triton X-100 for 5 minutes), blocked (2% bovine serum albumin [BSA]/5% horse serum [Life Technologies, Grand Island, NY] for 0.5 hour), and incubated for 1 hour with murine anti-PTPμ (BK2) antibodies (Santa Cruz) at 1:50 dilution followed by fluorescein isothiocyanate (FITC)-conjugated goat anti-mouse IgG (Molecular Probes, Eugene, OR) in 0.1% BSA in PBS as described [36]. The nuclei were counter-stained with 4′,6-diamidino-2-phenylindole (DAPI). After multiple washes, the monolayers were processed for standard fluorescence microscopy.

Epithelial wounding assay

A549 cells and SAECs were transfected with either PTPμ-targeting or control siRNAs, or infected with either Ad-PTPμ or an Ad-null vector control at an MOI of 100. Cells were cultured to confluence in the wells of 6-well plates (Corning, Corning, NY) and serum-starved for 4 to 6 hours. Using a sterile 200 μL pipette tip, a single wound was made across the diameter of each monolayer, after which cell debris was removed by washing with HEPES as described [42]. The A549 cells were then incubated for 24 hours, and the SAECs for 6 hours, with EGF (100 ng/mL or 1.67 nM) or medium alone. At 0 hour and either 6 or 24 hours, images of each monolayer were captured using a Nikon Eclipse TS100 microscope coupled to a Nikon Cool pix 4300 camera. Cell migration into the wound was calculated using ImageJ Software (Rasband, WS, ImageJ, US National Institutes of Health, Bethesda, MD; http://rsb.info.nih.gov/ij/). Cell migration into a wound after 6 and 24 hours was compared to that observed in the same wounded monolayer at 0 hour.

Epithelial cell chemotaxis assay

Gelatin-impregnated polycarbonate filters (13 mm diameter, 8.0 μm pore size; Nucleopore, Pleasanton, CA) were mounted in chemotactic chambers (Neuroprobe, Gaithersburg, MD) as described [43]. A549 cells transfected with either PTPμ-targeting or control siRNAs, or infected with either Ad-PTPμ or an Ad-null vector control at an MOI of 100, were added to the upper compartment of each assay chamber (2.0×10^5 cells in 0.8 mL). For the siRNA experiments, each lower compartment contained EGF 1 ng/mL and 0.1% fetal bovine serum (FBS) as the chemoattractants. For the Ad infection experiments, each lower compartment contained EGF 10 ng/mL and 0.1% FBS. After 5 hours' incubation (37°C, 5% CO_2), filters were removed, fixed (3.7% formaldehyde in PBS, 20 minutes), washed, stained with crystal violet, washed, and the top surface of each filter scraped free of cells. The crystal violet was then extracted from each filter with 0.1 M citric acid in 50% ethanol for 5 minutes and the absorbance at 560 nm (A_{560nm}) of extracts measured.

Statistics

For those outcomes measured once per sample, a Student's *t* test was used to compare experimental versus control groups. For those outcomes measured more than once per sample, a repeated measures analysis of variance (ANOVA) was applied using SAS PROC MIXED with a random effects model (random intercept) and an unstructured covariance matrix to account for the serial autocorrelation of repeated measures from the same sample. A 2-tailed $P < .05$ was considered significant.

RESULTS

PTPμ expression in human respiratory epithelia

To establish whether PTPμ is expressed at the protein level in epithelial cells derived from distinct regions of the human airway, confluent epithelia derived from the trachea (1HAEo$^-$ cells), bronchus (16HBE14o$^-$ and BEAS-2B cells), small airways (SAECs), and alveolus (A549 cells) were lysed and equal protein aliquots processed for PTPμ immunoblotting (Figure 1A). PTPμ-immunoreactive bands reflecting both full-length (~200-kDa) and proteolytically processed (~100-kDa) forms were detected in all 5 respiratory epithelia tested. The 100-kDa PTPμ cleavage products recognized by anti-PTPμ anti-bodies have been previously described in detail [29, 35, 38, 44–46]. After normalization to β-tubulin, the highest levels of PTPμ expression were seen in A549 cells (lane 1). PTPμ expression in SAECs was ~50% of that seen in A549 cells (lane 5) and that seen in BEAS-2B cells (lane 2), 1HAEo$^-$ cells (lane 3), and 16HBE14o$^-$ cells (lane 4) was 32%, 36%, and 39%, respectively. It is conceivable that the apparent differences between relative abundance of the 100-kDa form in the various cell lines may be explained through differential proteolytic processing.

Epithelial injury reduces PTPμ expression

Epithelial injury can disrupt cell-cell interactions and the epithelial barrier [5]. Adenoviruses utilize multiple host cell receptors for attachment and internalization [47], and are known to elicit tyrosine phosphorylation signaling events [48, 49]. Confluent A549 cells were infected with an Ad vector expressing GFP (Ad-GFP) with an MOI of 250 or incubated with medium alone for increasing times (1 to 6 days), after which cells were processed for PTPμ immunoblotting (Figure 1B). Over time, PTPμ protein expression was dramatically reduced in Ad-infected cells compared to the medium controls. By day 1, not only was full-length PTPμ (200-kDa) decreased, but also the proteolytically processed forms (~100-kDa) were substantially diminished (lanes 1 and 2). By days 4 to 5, full-length PTPμ was essentially undetectable in Ad-infected cells (lanes 8 and 10). The reduced PTPμ expression in Ad-

infected cells could not be explained through global protein synthesis inhibition; after normalization to β-tubulin, the decrease in PTPμ expression persisted (Figure 1B). The normalized PTPμ protein bands in Ad-infected cells compared to that seen in the simultaneous controls were reduced ~60% on day 1, ~40% on day 2, ~50% on day 3, ~60% on day 4, and >80% on day 5 ($n = 3$). We asked whether decreased PTPμ expression was specific to Ad infection or could result from other forms of injury. A549 cells exposed to H_2O_2, TNFα, heat shock, or hyperosmolarity all displayed a variable reduction of PTPμ expression (Figure 1C). In H_2O_2-treated cells, normalized PTPμ expression was reduced ~65% ($n = 20$) (lane 2 vs 1), in TNFα-treated cells, ~45% ($n = 3$) (lane 4 vs 3), after heat shock, ~25% ($n = 2$) (lane 8 vs 7), and after hyperosmolar stress, ~35% ($n = 18$) (lane 10 vs 9). After exposure to H_2O_2, the ~100-kDa band appeared as a doublet (lane 2). It is conceivable that this altered gel mobility results from oxidation of PTPμ as has been described [27]. In contrast, the relative abundance of PTPμ protein in LPS-exposed cells was not diminished ($n = 3$) (lane 6 vs 5).

The ectodomains of PTPμ expressed on neighboring cells extend into the paracellular space where they participate in strict homophilic adhesion [32]. Here, PTPμ remains trapped at the intercellular boundaries where its half-life is prolonged [38, 46]. To address whether the reduction of PTPμ expression in Ad-infected cells could be explained through loss of cell-cell contacts, confluent and subconfluent non-infected cells were analyzed for PTPμ expression (Figure 2). Using fluorescence microscopy to detect and immunolocalize PTPμ in confluent A549 cells, PTPμ staining was robust and found throughout the cytoplasm (Figure 2A, panel iii). In the subconfluent state, diminished PTPμ staining was detected in the perinuclear region (Figure 2A, panel iv). Similar to what was found in Ad-infected cells (Figure 1B), PTPμ expression was markedly reduced in the lysates of subconfluent cells compared to confluent cells (>50% reduced, $n = 23$) (Figure 2B; lane 2 vs 1). Again, full-length PTPμ (~200-kDa) was undetectable in subconfluent cells and the proteolytically processed forms (~100-kDa) were reduced. These combined data indicate that PTPμ protein expression is elevated in confluent, contact-inhibited cells and reduced coincident with loss of cell-cell contacts.

PTPμ counterregulates tyrosine phosphorylation of EGFR

A number of receptor and nonreceptor PTPs are known to dephosphorylate tyrosine residues within receptor PTKs, including EGFR [23, 24, 26, 27]. We asked whether PTPμ might influence EGFR autophosphorylation in lung epithelial cells. High PTPμ-expressing confluent A549 cells were transfected with either PTPμ-targeting or control siRNAs, and after 48 hours, were lysed, and the lysates processed for PTPμ immunoblotting (Figure 3A). After transfection with PTPμ-targeting siRNAs, full-length PTPμ and its proteolytically processed forms were all reduced to almost undetectable levels (Figure 3A, lane 2). Further, siRNA-induced knockdown of PTPμ did not alter protein expression of either of 2 full-length PTPs highly homologous to PTPμ, PTPκ, and PTPλ (Figure 3B). To determine whether such decreases in the level of PTPμ expression influenced EGFR expression, or conversely, whether the level of EGFR expression influenced PTPμ expression, the effect of siRNA-induced knockdown of each protein on expression of the other protein was defined (Figure 3C). After knockdown of PTPμ, EGFR protein expression was unchanged and after knockdown of EGFR, PTPμ protein expression remained unchanged. To establish whether PTPμ might regulate EGFR tyrosine autophosphorylation, A549 cells transfected with PTPμ-targeting or control siRNAs were exposed for 10 minutes to EGF (100 ng/mL) or medium alone, and were processed for phospho-EGFR immunoblotting with antibodies that recognize specific EGFR phosphotyrosines (PY845, PY992, PY1045, PY1068, PY1086, PY1148, or PY1173) ($n \geq 3$) (Figure 3D). Under un-stimulated conditions, PTPμ knockdown increased phosphorylation of Y992 ~10-fold and Y1068 >20-fold (lanes 1 and

2). Under these basal conditions, no changes in signal for PY845, PY1045, PY1086, PY1148, or PY1173 were detected. In control siRNA-transfected cells, the increases in phosphorylation of several tyrosine residues, Y1068 and Y1173, in response to EGF was minimal (lane 3 vs lane 1). In response to the EGF stimulus, PTPμ knockdown increased phosphorylation of Y845 (8.8-fold), Y992 (8.0-fold), Y1045 (4.5-fold), Y1068 (14-fold), Y1086 (3.5-fold), and Y1173 (3.0-fold), but not of Y1148 (1.1-fold) (lanes 3 and 4). Of interest, Y845 is not an autophosphorylation site but rather a phosphorylation site for src family PTKs [18]. It is conceivable that PTPμ might also influence src signaling. Transient infection of A549 cells with increasing MOIs of Ad-PTPμ resulted in dose-dependent overexpression of PTPμ normalized to β-tubulin from 5.7-fold (lane 2 vs 1) to 117-fold (lane 6 vs 1) (Figure 4A). In these same cells, EGFR expression remained unchanged. The effect of PTPμ overexpression on Y992 and Y1068 phosphorylation was assessed (Figure 4B, C). Overexpression of PTPμ in EGF-treated cells decreased EGFR autophosphorylation of both Y992 (58% reduction) (Figure 4B, lane 4 vs 3) and Y1068 (42% reduction) (Figure 4C, lane 4 vs 3). However, these decreases relative to the Ad-null control were far less than were the increases seen after PTPμ knockdown relative to the siRNA control (Figure 3D). Further, PTPμ overexpression did not decrease phosphorylation of other EGFR tyrosine residues tested (data not shown). These combined data indicate that in lung epithelial cells, especially in the presence of EGF stimulation, PTPμ selectively restrains phosphorylation of EGFR Y845, Y992, Y1045, Y1068, Y1086, and Y1173, but not of Y1148. Clearly, PTPμ depletion more readily altered EGFR autophosphorylation than did PTPμ overexpression.

The effect of PTPμ expression on EGFR Y1086 and Y992 phosphorylation and ERK1/2 and PLCγ activation

PTPμ restrains phosphorylation of specific tyrosine residues within EGFR (Figures 3D and 4B–C) and the phosphorylation state of each tyrosine is coupled to recruitment and activation of downstream signaling molecules [18]. EGFR autophosphorylation of Y1086 provides the dominant but not exclusive docking site for the adaptor molecule Shc, which can, through its interaction with Grb2, elicit ERK1/2 activation [18]. These signaling intermediates participate in the key cellular functions of proliferation and survival, 2 processes that contribute to epithelial repair and restitution [1]. Accordingly, A549 cells transfected with either PTPμ-targeting or control siRNAs were incubated for increasing times with EGF, after which they were processed for phospho-EGFR Y1086 immunoblotting (Figure 5A). PTPμ knockdown increased Y1086 phosphorylation relative to the simultaneous controls in response to the EGF stimulus, 1.7-fold (lane 2 vs 1) to 5.5-fold (lane 10 vs 9), at 2, 5, 20, 40, and 60 minutes. The EGF-induced increase in PY1086 signal was transient in that it decreased at ≥20 minutes (lanes 9, 11, and 13). In PTPμ-depleted cells, the PY1086 signal was more sustained and did not decrease until 60 minutes (lane 14). Under identical conditions, A549 cells were studied for ERK1/2 activation (Figure 5B). Although EGF increased phospho-ERK1/2 levels within 10 minutes, PTPμ knockdown was not associated with any further increases in ERK1/2 phosphorylation.

EGFR autophosphorylation of Y992 provides a docking site for PLCγ [18, 19] whose activation is a prerequisite to EGFR-mediated cell migration [10, 11]. Again, A549 cells were transfected with either PTPμ-targeting or control siRNAs and exposed for increasing times to EGF. Here, the cells were studied for EGFR Y992 phosphorylation (Figure 5C) and PLCγ_1 activation (Figure 5D). PTPμ knockdown was associated with increased Y992 phosphorylation relative to the simultaneous controls in response to the EGF stimulus, 1.4-fold (lane 2 vs 1) to 9-fold (lane 14 vs 13), at 2, 5, 10, 20, and 60 minutes (Figure 5C). These increases in Y992 phosphorylation paralleled increases in PLCγ_1 phosphorylation, 1.7-fold (lane 6 vs 5) to >5.0-fold (lane 4 vs 3), at 2 to 60 minutes (Figure 5D). Over this same time period, β-tubulin (Figure 5C) and total PCLγ1 protein (Figure 5D) expression remain

unchanged. These data indicate that PTPμ restrains EGFR Y992 phosphorylation, which, in turn, limits PCLγ1 activation, a key regulator of cell migration. Although PTPμ overexpression diminished Y992 phosphorylation (Figure 4B), it did not consistently diminish PLCγ1 phosphorylation (data not shown).

PTPμ restrains EGFR-driven A549 cell migration in wounding assay

Since PTPμ knockdown increases autophosphorylation of both EGFR Y992 and Y1173, the docking sites for PLCγ_1, and activation of PLCγ itself (Figure 5D), whereas PTPμ overexpression diminishes Y992 phosphorylation (Figure 4B), we asked whether changes in PTPμ expression could be coupled to increases in the EGFR-driven migratory response. A549 cells transfected with either PTPμ-targeting or control siRNAs, or transiently infected with Ad-PTPμ or Ad-null, were studied in the presence or absence of EGF for migration in a wounding assay. In this assay, cell migration into a wound was calculated as the area across which cells moved over 24 hours relative to 0 hour for the same monolayer, using ImageJ software. Representative results for one knockdown (Figure 6A) and one overexpression (Figure 6C) experiment are presented. Mean (± SE) migration for each of the experimental and control groups were quantified (Figure 6B and D). In cells transfected with either PTPμ-targeting or control siRNAs, EGF modestly increased cell migration compared to the simultaneous medium control. Under basal conditions, PTPμ knockdown increased cell migration by 23.4% compared to control siRNA-transfected cells ($n = 5$) but this increase did not quite attain statistical significance ($P = .054$). However, PTPμ knockdown in EGF-stimulated cells increased cell migration by 29% ($n = 5$; $P < .04$). Therefore, PTPμ restrains EGF-driven cell migration. In cells transiently infected with either Ad-PTPμ or Ad-null, again, EGF increased cell migration compared to the simultaneous medium control. Under basal conditions, PTPμ overexpression was not associated with any alterations in cell migration. In EGF-stimulated cells, although PTPμ overexpression diminished mean cell migration by 20% ($n = 4$), this decrease did not attain statistical significance ($P = .19$). These studies indicate that diminished levels of PTPμ expression influence the number of A549 cells that appear in the wound. That PTPμ overexpression was not associated with altered cell migration would suggest that once PTPμ expression exceeds a given threshold, further tyrosine dephosphorylation does not occur, or if it does, it is not coupled to changes in the migratory response. That PTPμ might increase cell numbers in the wound through increases in proliferation was excluded with cell counts in triplicate over 24 hours (data not shown). These combined data indicate that PTPμ restrains A549 cell migration in response to an EGF stimulus.

PTPμ restrains EGFR-driven A549 cell migration in a chemotaxis assay

Since cells must first reduce cell-cell contact with neighboring cells at the wound margin to migrate, and PTPμ is known to associate with and dephosphorylate ZA proteins [36], we asked whether PTPμ might also directly influence cell motility. Unattached suspended A549 cells, transfected with either PTPμ-targeting or control siRNAs, or transiently infected with Ad-PTPμ or Ad-null, were studied in the presence or absence of EGF for migration in a chemotaxis assay (Figure 7). In cells transfected with either PTPμ-targeting ($P < .004$) or control siRNAs ($P < .06$), EGF modestly increased cell migration compared to the simultaneous medium controls. Under basal conditions, PTPμ knockdown was not associated with altered cell migration ($n = 13$). In EGF-stimulated cells, PTPμ knockdown increased cell migration by 18.3% ($n = 13$) ($P < .03$). In cells transiently infected with either Ad-PTPμ or Ad-null, again, EGF modestly increased cell migration compared to the simultaneous medium control. In these same cells, PTPμ overexpression diminished cell migration by 11.5% ($n = 17$) ($P < .05$). In the presence of EGF, PTPμ overexpression decreased cell migration by 9.0% ($n = 17$), but this decrease did not reach statistical significance ($P = .18$). These combined data indicate that in suspended nonadherent

epithelial cells, PTPμ expression, within physiological ranges, regulates EGFR-driven cell motility. However, supraphysiological levels of PTPμ did not further alter EGF-stimulated migration.

PTPμ restrains EGFR-driven SAEC migration in wounding assay

PTPμ is expressed in both A549 cells and SAECs (Figure 1A). PTPμ depletion in A549 cells enhances cell migration (Figures 6A–B and 7A). Since A549 cells are transformed tumor cells, we asked whether human primary SAECs might similarly respond to PTPμ depletion in the wounding assay (Figure 8). SAECs were transfected with either PTPμ-targeting or control siRNAs, cultured to confluence, lysed, and the lysates processed for PTPμ immunoblotting (Figure 8A). In SAECs, PTPμ was knocked down >80%. In other experiments, confluent cells were wounded and cultured for 6 hours in the presence or absence of EGF (100 ng/mL) (Figure 8B–C). In cells transfected with either PTPμ-targeting or control siRNAs, EGF increased cell migration compared to the simultaneous medium control (Figure 8C). The SAECs migrated more in 6 hours (Figure 8C) than did A549 cells over 24 hours (Figure 6B). Further, the SAECs were more EGF responsive. In the absence of EGF stimulation, PTPμ knockdown increased cell migration by >2.0-fold compared to control siRNA-transfected cells ($n = 6$; $P < .0001$) (Figure 8C). PTPμ knockdown in EGF-stimulated cells increased cell migration, again, by >2.0-fold ($n = 6$; $P < .0001$) (Figure 8C). Since the wounding assays with SAECs were all performed within 6 hour, the increased cells within the wound, again, could not be explained through cell proliferation. Therefore, PTPμ depletion in primary human SAECs enhances cell migration under basal conditions and, to a greater extent, in response to the EGF stimulus. These combined data (Figures 6–8) indicate that PTPμ restrains SAEC migration under basal conditions, whereas it counterregulates migration of both A549 cells and SAECs in response to the EGF stimulus. Of note, the influence of PTPμ on the EGFR-driven migratory response in the more clinically relevant primary respiratory epithelia (Figure 8) was more robust than that seen in transformed A549 cells (Figures 6–7).

DISCUSSION

In these studies, PTPμ protein was detected in lung airway epithelia (Figure 1A). In these same cells, diverse forms of injury (Figure 1B–C) and subconfluent growth (Figure 2B) each dramatically reduced PTPμ expression. PTPμ knockdown was associated with increased EGFR tyrosine phosphorylation (Figure 3D). Under basal conditions, PTPμ knockdown selectively increased EGFR phosphorylation of Y992 and Y1068 (lanes 1 and 2). In response to an EGF stimulus, PTPμ knockdown selectively increased phosphorylation of Y845, Y992, Y1045, Y1068, Y1086, and Y1173 (lanes 3 and 4). Such manipulation of PTPμ expression did not alter EGFR expression (Figure 3C). Conversely, ectopic PTPμ overexpression decreased Y992 and Y1068 phosphorylation (Figure 4B–C). In the presence of EGF, PTPμ knockdown increased and sustained both Y992 phosphorylation and PLCγ_1 activation over time (Figure 5C–D). Finally, in both wounding and chemotaxis assays, PTPμ knockdown modestly increased EGFR-driven migration of A549 cells (Figures 6–7) and, to a greater extent, migration of the more clinically relevant SAECs (Figure 8).

Ad is a nonenveloped, double-stranded DNA virus that recognizes multiple receptors that dictate tissue tropism, virus entry, intracellular signaling, and the host cell response [47]. Selected Ad-host receptor interactions can be coupled to tyrosine phosphorylation events, including activation of c-src, ERK1/2, and focal adhesion kinase [48, 49]. Since Ad infection markedly reduced PTPμ expression (Figure 1B), it is conceivable that one or more of these Ad-induced tyrosine phosphorylation events may be amplified and/or stabilized. We then asked whether other forms of airway epithelial injury might also reduce PTPμ expression. Diverse injurious stimuli, including oxidant stress with H_2O_2, exposure to the

proinflammatory cytokine, TNFα, and hyperthermia and hyperosmolar conditions, all reduced PTPμ expression (Figure 1C). However, a challenge with bacterial LPS did not. LPS is known, through the Toll-like receptor 4 pathway, to transcriptionally activate multiple downstream genes [50]. Whether PTPμ might be one of these up-regulated gene products is unknown. Of interest, H_2O_2, TNFα, heat shock, and hyperosmotic conditions each are known to transactivate EGFR [51, 52], whereas LPS does not (S.E.G., unpublished data). Whether the ability of a specific injurious stimulus to reduce PTPμ expression can be coupled to its ability to activate EGFR is unclear. In fact, EGFR signaling has been shown to downregulate another receptor PTP, LAR (Leukocyte Common Antigen Related)-PTP, through TNFα converting enzyme-mediated proteolysis [53]. PTPμ is proteolytically processed by proprotein convertase (PC)5, a member of the subtilisin/kexin-like PC family [38] as well as another family member, furin, together with ADAM (A Disintegrin And Metalloproteinase)10, followed by intramembranous cleavage through γ-secretase activity [44]. Receptor PTPs have been classified into 8 distinct subfamilies based on the similarity of their extracellular domains [30]. PTPμ belongs to the type IIb subfamily whose members each contain an NH_2-terminal MAM domain together with Ig-like and FN type III domains [29, 30]. This group includes PTPμ, PTPκ, PTPλ, PCP2, and PTPρ. Like PTPμ, a number of these PTPs each contain a target motif (RXK/RR) recognized by the subtilisin/kexin-like endoproteases [38]. Whether the reduction of PTPμ expression in response to these injurious stimuli can be explained through EGFR activation and/or proteolytic processing and/or whether other related receptor PTPs might be similarly reduced is unclear and currently under study.

As cell density increases, the relative abundance of full-length PTPμ protein increases (Figure 2B) [38]. At confluence, the 200-kDa PTPμ species increases ~4-fold relative to its expression under subconfluent conditions. Opposing PTPμ ectodomains on neighboring cells homophilically interact [32], whereas the cytoplasmic domain directly associates with cell-cell adherens junctions through the cadherins [35, 36, 45]. These homophilic and heterophilic interactions trap PTPμ at the cell-cell interface where its half-life is markedly prolonged [38, 46]. Since cell-cell contact is associated with dramatic increases in PTPμ protein [38], we asked whether the reduction of PTPμ in response to injury might be mediated through loss of cell-cell contacts. To address this question, the relative abundance of PTPμ protein in subconfluent cells was compared to confluent cells. Subconfluent cells displayed a reduction in PTPμ expression relative to that seen under confluent conditions (Figure 2B) that was comparable to that seen with injury (Figure 1B and C). It is conceivable that loss of homophilic interaction between PTPμ ectodomains serves as the biological switch for decreased PTPμ protein expression. Similarly, other homophilically adhering, membrane-spanning, junctional proteins that extend into and across the paracellular space, such as the cadherins, might also participate [54]. Differentiated human airway epithelia are quiescent with a low rate of cell division [5]. Under resting conditions, the tight junctions of these polarized and contact-inhibited cells segregate apical and basolateral membranes, including the membrane-spanning ErbB proligands and ErbB receptors they contain [5]. In response to injury where cell-cell contact is lost, ErbB ligands gain access to and activate ErbB receptors [5]. We now have demonstrated that coincident with loss of cell-cell contacts and ErbB receptor activation, PTPμ expression is reduced (Figure 2B) and EGFR receptor phosphorylation (Figure 3D) and downstream signaling (Figure 5D) amplified. It is conceivable that during the airway epithelial response to diverse forms of injury, in which cell-cell integrity is mechanically or biochemically perturbed, PTPμ expression is reduced so as to amplify the tyrosine phosphorylation events required for epithelial restitution and repair. Whether this PTPμ depletion provoked by injury can be explained through changes in transcription and/or translation is unknown and is currently under study.

Upon activation, EGFR homo- and heterodimerizes with other ErbB receptors [18]. The kinase domain of each of these receptors phosphorylates tyrosine residues within the cytoplasmic portion of its ErbB binding partner. At the same time, other PTKs, such as SFKs and Jak-2, also phosphorylate tyrosines within these same receptors. Upon phosphorylation, these tyrosines provide docking sites for signaling molecules containing SH2- and phosphotyrosine-binding domains, the recruitment of which is coupled to downstream signaling pathways and cell responses [18]. Knockdown of PTPμ selectively increased phosphorylation of Y845, Y992, Y1045, Y1068, Y1086, and Y1173 (Figure 3D), whereas PTPμ overexpression decreased Y992 and Y1068 phosphorylation (Figure 4B–C). Phosphotyrosines PY1068 and PY1086 can serve as docking sites for the adapter protein, Grb-2, which participates in ERK1/2 activation [18]. Although PTPμ knockdown increased Y1086 phosphorylation over a sustained (≥1 hour) period (Figure 5A), over this same time, no increase in ERK1/2 activation was detected (Figure 5B). Over this same time period, PTPμ knockdown also increased phosphorylation of Y992 (Figure 5C), the docking site for PLCγ_1 [18, 19], as well activation of PLCγ_1 itself (Figure 5D), a prerequisite signaling event essential to EGFR-driven epithelial cell migration [10, 11]. Just as PTPμ knockdown in the presence of EGF increased Y992 phosphorylation (Figures 3D and 5C), PTPμ knockdown increased cell migration in response to the EGF stimulus (Figures 6B, 7A, and 8C). Although not tested in these studies, PTPμ might also influence signaling events downstream to PLCγ_1, including PIP_2 hydrolysis, generation of IP3 and DAG, increases in cytosolic Ca^{2+}, and PKC activation [20, 21]. It is also possible that PTPμ depletion might play a permissive role for migration through cadherin and/or catenin tyrosine hyper-phosphorylation and adherens junction disassembly [36]. Finally, PTPμ depletion was far more efficient at increasing EGFR and PLCγ phosphorylation (Figures 3D and 5D) than PTPμ overexpression was at decreasing either event (Figure 4B–C and data not shown). These results are consistent with the greater ability of PTPμ depletion to increase A549 cell migration (Figures 6B and 7A) than could PTPμ overexpression diminish it (Figures 6D and 7B). That PTPμ overexpression was not associated with altered cell migration would suggest that once PTPμ expression exceeds a given threshold, further tyrosine dephosphorylation does not occur, or if it does, it is not coupled to changes in the migratory response.

In summary, EGFR activation is a key component to the airway epithelial response to disruptive denuding injury. First, EGFR ligands, such as TGFα, are increased in both the lungs of experimental animals [55] and the pulmonary edema fluids of patients [56, 57] with acute lung injury. Further, a wide range of diverse injurious stimuli can activate EGFR, including heat shock [51], ultraviolet (UV) and γ radiation [51, 58, 59], oxidant stress with H_2O_2 [51], heavy metals [59], alkylating agents [51], hyperosmotic conditions [51], as well as the endogenous mediators, thrombin [60], TNFα [52], and platelet-activating factor [61]. As cell-cell integrity is compromised, intercellular junctions are disassembled and EGFR ligands permitted access to their respective receptors [5]. The current studies indicate that a component of the host repair program elicited by a disruptive epithelial cell injury is a coordinate reduction of PTPμ expression. This diminished PTPμ activity permits hyperphosphorylation of specific EGFR tyrosines, including the docking sites for PLCγ_1, sustained PLCγ activation, and a modestly increased migratory cellular response. The EGFR-mediated migratory response studied here was driven by EGF, only 1 of at least 7 known high-affinity EGFR ligands [62]. In the intact lung, where multiple EGFR ligands are coexpressed, the EGFR-driven epithelial repair program and its response to PTPμ counterregulation may be more robust. Further, other MAM domain-containing homophilically interacting receptor PTPs [39, 40, 63], like PTPμ, may also be reduced in response to epithelial injury. EGFR activation in concert with reduced PTPμ expression may be a pivotal component in a final common pathway for the host response to a subset of injurious stimuli leading to acute airway epithelial injury.

Acknowledgments

This work was supported by grants from the National Institutes of Health, including HL084223 and HL070155 (S.E.G.), GM55989 (N.K.T.), and P30-AG028747 (J.D.S.). The authors thank Ms. Shirley Taylor for excellent secretarial support.

References

1. Burgel PR, Nadel JA. Roles of epidermal growth factor receptor activation in epithelial cell repair and mucin production in airway epithelium. Thorax. 2004; 59:992–996. [PubMed: 15516478]
2. Barrow RE, Wang CZ, Evans MJ, Herndon DN. Growth factors accelerate epithelial repair in sheep trachea. Lung. 1993; 171:335–344. [PubMed: 8295428]
3. Kheradmand F, Folkesson HG, Shum L, Derynk R, Pytela R, Matthay MA. Transforming growth factor-alpha enhances alveolar epithelial cell repair in a new in vitro model. Am J Physiol. 1994; 267:L728–738. [PubMed: 7810677]
4. Godfrey RW. Human airway epithelial tight junctions. Microsc Res Tech. 1997; 38:488–499. [PubMed: 9376652]
5. Vermeer PD, Einwalter LA, Moninger TO, Rokhlina T, Kern JA, Zabner J, Welsh MJ. Segregation of receptor and ligand regulates activation of epithelial growth factor receptor. Nature. 2003; 422:322–326. [PubMed: 12646923]
6. Takeichi M. Cadherins in cancer. implications for invasion and metastasis. Curr Opin Cell Biol. 1993; 5:806–811. [PubMed: 8240824]
7. Kim JS, McKinnis VS, Nawrocki A, White SR. Stimulation of migration and wound repair of guinea-pig airway epithelial cells in response to epidermal growth factor. Am J Respir Cell Mol Biol. 1998; 18:66–74. [PubMed: 9448047]
8. Burgel PR, Escudier E, Coste A, Dao-Pick T, Ueki IF, Takeyama K, Shim JJ, Murr AH, Nadel JA. Relation of epidermal growth factor receptor expression to goblet cell hyperplasia in nasal polyps. J Allergy Clin Immunol. 2000; 06:705–712. [PubMed: 11031341]
9. Takeyama K, Fahy JV, Nadel JA. Relationship of epidermal growth factor receptors to goblet cell production in human bronchi. Am J Respir Crit Care Med. 2001; 163:511–516. [PubMed: 11179132]
10. Chen P, Xie H, Sekar MC, Gupta K, Wells A. Epidermal growth factor receptor-mediated cell motility. phospholipase C activity is required. but mitogen-activated protein kinase activity is not sufficient for induced cell movement. J Cell Biol. 1994; 127:847–857. [PubMed: 7962064]
11. Xie H, Pallero MA, Gupta K, Chang P, Ware MF, Witke W, Kwiatkowski DJ, Lauffenburger DA, Murphy-Ullrich JE, Wells A. EGF receptor regulation of cell motility. EGF induces disassembly of focal adhesions independently of the motility-associated PLCgamma signaling pathway. J Cell Sci. 1998; 111:615–624. [PubMed: 9454735]
12. Chen P, Murphy-Ullrich JE, Wells A. A role for gelsolin in actuating epidermal growth factor receptor-mediated cell motility. J Cell Biol. 1996; 134:689–698. [PubMed: 8707848]
13. Malliri A, Symons M, Hennigan RF, Hurlstone AFL, Lamb RF, Wheeler T, Ozanne BW. The transcription factor AP-1 is required for EGF-induced activation of rho-like GTPases. cytoskeletal rearrangements. motility. and in vitro invasion of A431 cells. J Cell Biol. 1998; 143:1087–1099. [PubMed: 9817764]
14. Hoschuetzky H, Aberle H, Kemler R. Beta-catenin mediates the interaction of the cadherin-catenin complex with epidermal growth factor receptor. J Cell Biol. 1994; 127:1375–1380. [PubMed: 7962096]
15. Mariner DJ, Davis MA, Reynolds AB. EGFR signaling to p120-catenin through phosphorylation at Y228. J Cell Sci. 2004; 117:1339–1350. [PubMed: 14996911]
16. Shibamoto S, Hayakawa M, Takeuchi K, Hori T, Oku N, Miyazawa K, Kitamura N, Takeichi M, Ito F. Tyrosine phosphorylation of beta-catenin and plakoglobin enhanced by hepatocyte growth factor and epidermal growth factor in human carcinoma cells. Cell Adhes Commun. 1994; 1:295–305. [PubMed: 8081883]

17. Hamaguchi M, Matsuyoshi N, Ohnishi Y, Gotoh B, Takeichi M, Nagai Y. p60v-src causes tyrosine phosphorylation and inactivation of the N-cadherin-catenin cell adhesion system. EMBO J. 1993; 12:307–314. [PubMed: 8381351]
18. Olayioye MA, Neve RM, Lane HA, Hynes NE. The ErbB signaling network. receptor heterodimerization in development and cancer. EMBO J. 2000; 19:3159–3167. [PubMed: 10880430]
19. Chattopadhyay A, Vecchi M, Ji Q, Mernaugh R, Carpenter G. The role of individual SH2 domains in mdiating association of phospholipase C-gamma1 with the activated EGF receptor. J Biol Chem. 1999; 274:26091–26097. [PubMed: 10473558]
20. Carpenter G, Ji Q-S. Phospholipase C-γ as a signal-transducing element. Exp Cell Res. 1999; 253:15–24. [PubMed: 10579907]
21. Wells A, Grandis JR. Phospholipase C-γ_1 in tumor progression. Clin Exp Metastasis. 2003; 20:285–290. [PubMed: 12856715]
22. Tice DA, Biscardi JS, Nickles AL, Parsons SJ. Mechanism of biological synergy between cellular Src and epidermal growth factor receptor. Proc Natl Acad Sci U S A. 1999; 96:1415–1420. [PubMed: 9990038]
23. Deb TB, Wong L, Salomon DS, Zhou G, Dixon JE, Gutkind S, Thompson SA, Johnson GR. A common requirement for the catalytic activity and both SH2 domains of SHP-2 in mitogen-activated protein (MAP) kinase activation by the ErbB family of receptors. J Biol Chem. 1998; 273:16643–16646. [PubMed: 9642214]
24. Lee S-R, Kwon K-S, Kim S-R, Rhee SG. Reversible inactivation of protein-tyrosine phasphatase 1B and A431 cells stimulated with epidermal growth factor. J Biol Chem. 1998; 273:15366–15372. [PubMed: 9624118]
25. Xu Y, Tan LJ, Grachtchouk V, Voorhees JJ, Fisher GJ. Receptor-type protein-tyrosine phosphatase-kappa regulates epidermal growth factor receptor function. J Biol Chem. 2005; 280:42694–42700. [PubMed: 16263724]
26. Bae YS, Kang SW, Seo MS, Baines IC, Tekle E, Chock PB, Rhee SG. Epidermal growth factor (EGF)-induced generation of hydrogen perioxide. J Biol Chem. 1997; 272:217–221. [PubMed: 8995250]
27. Denu JM, Tanner KG. Specific and reversible inactivation of protein tyrosine phosphatases by hydrogen peroxide. evidence for a sulfenic acid intermediate and implications for redox regulation. Biochemistry. 1998; 37:5633–5642. [PubMed: 9548949]
28. Fuchs M, Wang H, Ciossek T, Chen Z, Ullrich A. Differential expression of MAM-subfamily protein tyrosine phosphatases during mouse development. Mech Dev. 1998; 70:91–109. [PubMed: 9510027]
29. Gebbink MF, van Etten I, Hateboer G, Suijkerbuijk R, Beijersbergen RL, Geurts van Kessel A, Moolenaar WH. Cloning. expression and chromosomal localization of a new putative receptor-like protein tyrosine phosphatase. FEBS Lett. 1991; 290:123–130. [PubMed: 1655529]
30. Brady-Kalnay SM, Tonks NK. Protein tyrosine phosphatases as adhesion receptors. Curr Opin Cell Biol. 1995; 7:L650–L657.
31. Aricescu AR, Hon WC, Siebold C, Lu W, van der Merwe PA, Jones EY. Molecular analysis of receptor protein tyrosine phosphatase mu-mediated cell adhesion. EMBO J. 2006; 25:701–712. [PubMed: 16456543]
32. Brady-Kalnay SM, Tonks NK. Identification of the homophilic binding site of the receptor protein tyrosine phosphatase PTPμ. J Biol Chem. 1994; 269:28472–28477. [PubMed: 7961788]
33. Cismasiu VB, Denes SA, Reiländer H, Michel H, Szedlacsek SE. The MAM (meprin/A5-protein/PTPmu) domain is a homophilic binding site promoting the lateral dimerization of receptor-like protein-tyrosine phosphatase mu. J Biol Chem. 2004; 279:26922–26931. [PubMed: 15084579]
34. Del Vecchio RL, Tonks NK. The conserved immunoglobulin domain controls the subcellular localization of the homophilic adhesion receptor protein-tyrosine phosphatase mu. J Biol Chem. 2005; 280:1603–1612. [PubMed: 15491993]
35. Brady-Kalnay SM, Mourton T, Nixon JP, Pietz GE, Kinch M, Chen H, Brackenbury R, Rimm DL, Del Vecchio RL, Tonks NK. Dynamic interaction of PTPμ with multiple cadherins in vivo. J Cell Biol. 1998; 141:287–296. [PubMed: 9531566]

36. Sui XF, Kiser TD, Hyun SW, Angelini DJ, Del Vecchio RL, Young BA, Hasday JD, Romer LH, Passaniti A, Tonks NK, Goldblum SE. Receptor protein tyrosine phosphatase micro regulates the paracellular pathway in human lung microvascular endothelia. Am J Pathol. 2005; 166:1247–1258. [PubMed: 15793303]
37. Zondag GC, Reynolds AB, Moolenaar WH. Receptor protein-tyrosine phosphatase RPTPmu binds to and dephosphorylates the catenin p120(ctn). J Biol Chem. 2000; 275:11264–11269. [PubMed: 10753936]
38. Campan M, Yoshizumi M, Seidah NG, Lee ME, Bianchi C, Haber E. Increased proteolytic processing of protein tyrosine phosphatase mu in confluent vascular endothelial cells. the role of PC5. a member of the subtilisin family. Biochemistry. 1996; 35:3797–3802. [PubMed: 8620001]
39. Sap J, Jiang YP, Friedlander D, Grumet M, Schlessinger J. Receptor tyrosine phosphatase R-PTP-kappa mediates homophilic binding. Mol Cell Biol. 1994; 14:1–9. [PubMed: 8264577]
40. Cheng J, Wu K, Armanini M, O'Rourke N, Dowbenko D, Lasky LA. A novel protein-tyrosine phosphatase related to the homotypically adhering kappa and mu receptors. J Biol Chem. 1997; 272:7264–7277. [PubMed: 9054423]
41. Kim JW, Sim SS, Kim U-H, Nishibe S, Wohl MI, Carpenter G, Rhee SG. Tyrosine residues in bovine phospholipase C-γ phosphorylated by the epidermal growth factor receptor *in vitro*. J Biol Chem. 1990; 265:3940–3943. [PubMed: 1689310]
42. Liu A, Garg P, Yang S, Gong P, Pallero MA, Annis DS, Liu Y, Passaniti A, Mann D, Mosher DF, Murphy-Ullrich JE, Goldblum SE. The EGF-like repeats of thrombospondins activate phospholipase C gamma and increase epithelial cell migration through indirect epidermal growth factor receptor activation. J Biol Chem. 2009; 284:6389–6402. [PubMed: 19129184]
43. Sun L, Vitolo M, Passaniti A. Runt-related gene 2 in endothelial cells. inducible expression and specific regulation of cell migration and invasion. Cancer Res. 2001; 61:4994–5001. [PubMed: 11431332]
44. Anders L, Mertins P, Lammich S, Murgia M, Hartmann D, Saftig P, Haass C, Ullrich A. Furin-. ADAM 10-. and gamma-secretase-mediated cleavage of a receptor tyrosine phosphatase and regulation of beta-catenin's transcriptional activity. Mol Cell Biol. 2006; 26:3917–3934. [PubMed: 16648485]
45. Brady-Kalnay SM, Rimm DL, Tonks NK. Receptor protein tyrosine phosphatase PTPmu associates with cadherins and catenins in vivo. J Cell Biol. 1995; 130:977–986. [PubMed: 7642713]
46. Gebbink MF, Zondag GC, Koningstein GM, Feiken E, Wubbolts RW, Moolenaar WH. Cell surface expression of receptor protein tyrosine phosphatase RPTPμ is regulated by cell-cell contact. J Cell Biol. 1995; 131:251–260. [PubMed: 7559782]
47. Zhang Y, Bergelson JM. Adenovirus receptors. J Virol. 2005; 79:12125–12131. [PubMed: 16160140]
48. Natarajan K, Ghalayini AJ, Sterling RS, Holbrook RM, Kennedy RC, Chodosh J. Activation of focal adhesion kinase in adenovirus-infected human corneal fibroblasts. Invest Ophthalmol Vis Sci. 2002; 43:2685–2690. [PubMed: 12147603]
49. Natarajan K, Rajala MS, Chodosh J. Corneal IL-8 expression following adenovirus infection is mediated by c-Src activation in human corneal fibroblasts. J Immunol. 2003; 170:6234–6243. [PubMed: 12794155]
50. Hashimoto S, Morohoshi K, Suzuki T, Matsushima K. Lipopolysaccharide-inducible gene expression profile in human monocytes. Scand J Infect Dis. 2003; 35:619–627. [PubMed: 14620145]
51. Carpenter G. Employment of the epidermal growth factor receptor in growth factor-independent signaling pathways. J Cell Biol. 1999; 146:697–702. [PubMed: 10459005]
52. Donato NJ, Gallick GE, Steck PA, Rosenblum MG. Tumor necrosis factor modulates epidermal growth factor receptor phosphorylation and kinase activity in human tumor cells. Correlation with cytotoxicity. J Biol Chem. 1989; 264:20474–20481. [PubMed: 2555361]
53. Ruhe JE, Streit S, Hart S, Ullrich A. EGFR signaling leads to downregulation of PTP-LAR via TACE-mediated proteolytic processing. Cell Signal. 2006; 18:1515–1527. [PubMed: 16478662]

54. Perez-Moreno M, Jamora C, Fuchs E. Sticky business. orchestrating cellular signals at adherens junctions. Cell. 2003; 112:535–548. [PubMed: 12600316]
55. Vivekananda J, Lin A, Coalson JJ, King RJ. Acute inflammatory injury in the lunch precipitated by oxidant stress induces fibroblasts to synthesize and release transforming growth factor-α. J Biol Chem. 1994; 269:25057–25061. [PubMed: 7929192]
56. Chesnutt AN, Kheradmand F, Folkesson HG, Alberts M, Matthay MA. Soluble transforming growth factor-α is present in the pulmonary edema fluid of patients with acute lung injury. Chest. 1997; 111:652–656. [PubMed: 9118703]
57. Madtes DK, Rubenfeld G, Klima LD, Milberg JA, Steinberg KP, Martin TR, Raghu G, Hudson LD, Clark JG. Elevated transforming growth factor-alpha levels in bronchoalveolar lavage fluid of patients with acute respiratory distress syndrome. Am J Respir Crit Care Med. 1998; 158:424–430. [PubMed: 9700116]
58. Bowers G, Reardon D, Hewitt T, Dent P, Mikkelsen RB, Valerie K, Lammering G, Amir C, Schmidt-Ullrich RK. The relative role of ErbB1–4 receptor tyrosine kinases in radiation signal transduction responses of human carcinoma cells. Oncogene. 2001; 20:1388–1397. [PubMed: 11313882]
59. Huang R-P, Wu J-X, Fan Y, Adamson ED. UV activates growth factor receptors via reactive oxygen intermediates. J Cell Biol. 1996; 133:211–220. [PubMed: 8601609]
60. Prenzel N, Zwick E, Daub H, Leserer M, Abraham R, Wallasch C, Ullrich A. EGF receptor transactivation by G-protein-coupled receptors requires metalloproteinase cleavage of proHB-EGF. Nature. 1999; 402:884–888. [PubMed: 10622253]
61. Pan Z, Kravchenko VV, Ye RD. Platelet-activating factor stimulates transcription of the heparin-binding epidermal growth factor-like growth factor in monocytes. J Biol Chem. 1995; 270:7787–7790. [PubMed: 7713868]
62. Harris RC, Chung E, Coffey RJ. EGF receptor ligands. Exp Cell Res. 2003; 284:2–13. [PubMed: 12648462]
63. McAndrew PE, Frostholm A, White RA, Rotter A, Burghes AHM. Identification and characterization of RPTP rho, a novel RPTP mu/kappa-like receptor protein tyrosine phosphatase whose expression is restricted to the central nervous system. Brain Res Mol Brain Res. 1998; 56:9–21. [PubMed: 9602027]

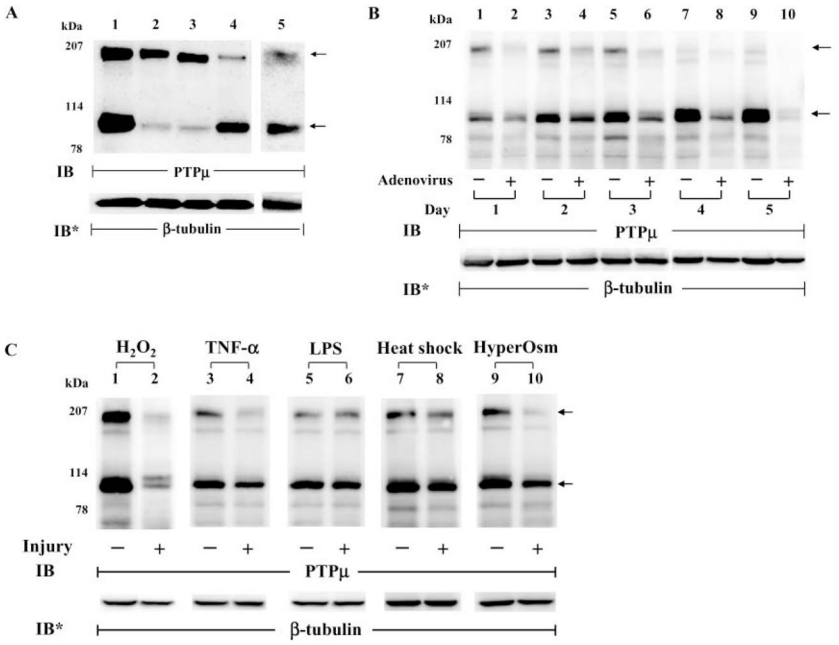

FIGURE 1.

Diverse injurious stimuli reduce PTPμ expression in human respiratory epithelia. (**A**) Postconfluent respiratory epithelia, including A549 cells (lane 1), BEAS-2B cells (lane 2), 1HAEo$^-$ cells (lane 3), 16HBE14o$^-$ cells (lane 4), and SAECs (lane 5), each were lysed and the lysates processed for immunoblotting with SK15 anti-PTPμ antibodies. (**B**) Confluent A549 cells were infected with Ad-GFP at an MOI of 250 or cultured in medium alone for 1 to 6 days. On days 1, 2, 3, 4, and 5, infected and control cells were lysed and the lysates processed for PTPμ immunoblotting. (**C**) Postconfluent A549 cells were exposed to H_2O_2 (5 mM, 48 hours), TNFα (200 ng/mL, 72 hours), LPS (100 μg/mL, 72 hours), heat shock (43°C, 1 hour), hyperosmolarity (200 mM NaCl, 24 hours), or medium alone. Cells were lysed and the lysates processed for PTPμ immunoblotting. To control for protein loading and transfer, blots were stripped and reprobed for β-tubulin. Molecular weight in kDa is indicated on left. Arrows on right indicate the full-length (~200-kDa) and proteolytically processed (~100-kDa) PTPμ immunoreactive bands. IB = immunoblot; IB* = immunoblot after stripping. Each blot is representative of ≥3 independent experiments.

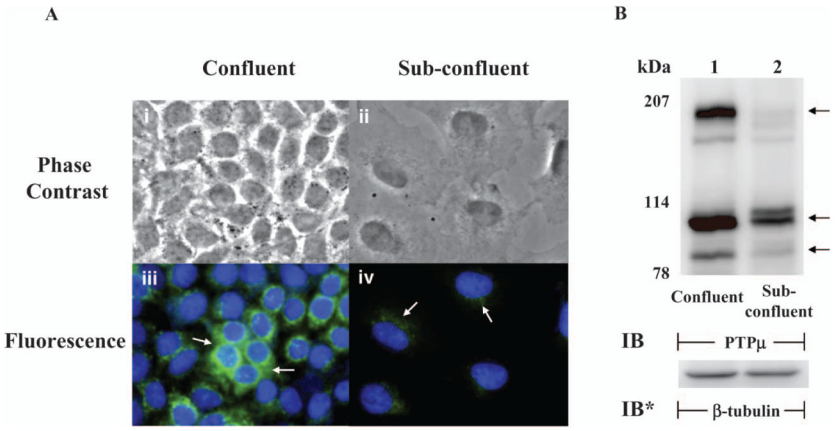

FIGURE 2.

Loss of cell confluence reduces PTPμ expression. A549 cells were seeded at 0.2×10^5 or 2×10^5 cells per well on coverslips in 6-well plates and cultured for 2 to 3 days to generate subconfluent and confluent monolayers. (**A**) Cells were fixed, permeabilized, and probed with murine BK2 anti-PTPμ antibodies followed by FITC-conjugated goat anti-mouse IgG for phase-contrast and fluorescence microscopy (400×). Nuclei were counterstained with DAPI. Arrows indicate PTPμ signal. (**B**) Confluent (lane 1) and subconfluent (lane 2) cells were lysed and the lysates processed for PTPμ immunoblotting. Blots were stripped and reprobed for β-tubulin. IB = immunoblot; IB* = immunoblot after stripping. Molecular weight in kDa is indicated on left. Arrows on right indicate PTPμ immunoreactive bands. Blot is representative of two independent experiments. (Color figure available online.)

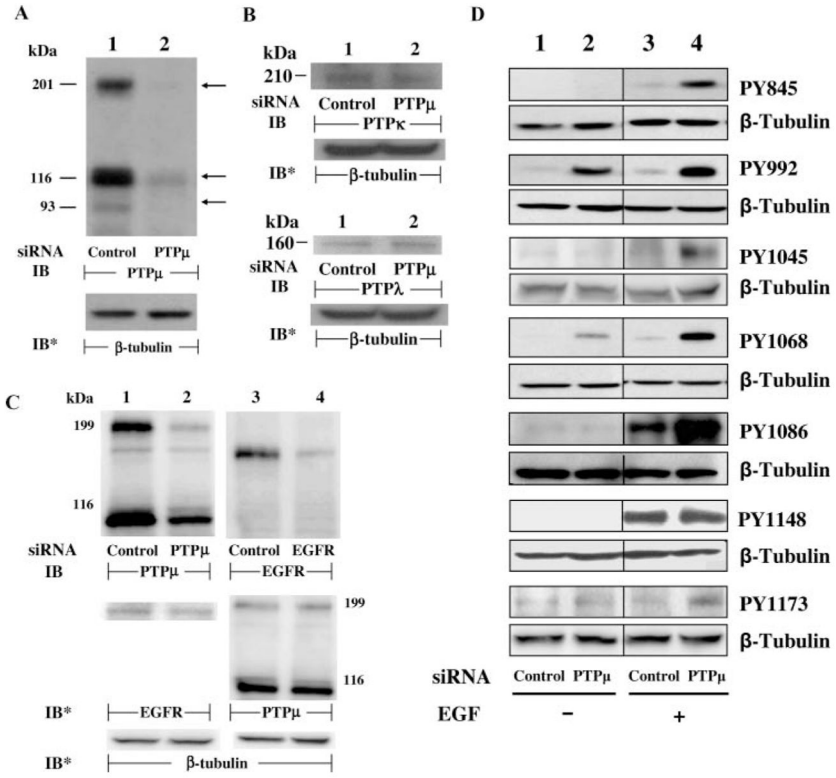

FIGURE 3.

siRNA-mediated knockdown of PTPμ increases EGF-stimulated EGFR tyrosine phosphorylation. (**A**) A549 cells at 80% confluence were transfected with control siRNA duplexes (lane 1) or PTPμ-targeting siRNAs (lane 2), lysed, and the lysates were processed for PTPμ immunoblotting. (**B**) A549 cells transfected with PTPμ-targeting or control siRNAs were processed for immunoblotting with anti-PTPκ and anti-PTPλ antibodies. (**C**) A549 cells were transfected with PTPμ-targeting, EGFR-targeting, or control siRNA duplexes, lysed, and the lysates processed for either PTPμ (lanes 1 and 2) or EGFR (lanes 3 and 4) immunoblotting. (**D**) A549 cells were transfected with control siRNA duplexes (lanes 1 and 3) or PTPμ-targeting siRNAs (lanes 2 and 4), after which they were serum starved for 24 hours and treated for 10 minutes with EGF (100 ng/mL) (lanes 3 and 4) or medium alone (lanes 1 and 2). Cells were lysed and the lysates processed for phospho-EGFR immunoblotting with antibodies to specific phosphotyrosine residues including PY845, PY992, PY1045, PY1068, PY1086, PY1148, and PY1173. To control for protein loading and transfer, blots were stripped and reprobed for β-tubulin. In **A**, **B**, and **C**, IB = immunoblot and IB* = immunoblot after stripping. Molecular weight in kDa indicated on left of blot. These blots are representative of ≥3 independent experiments.

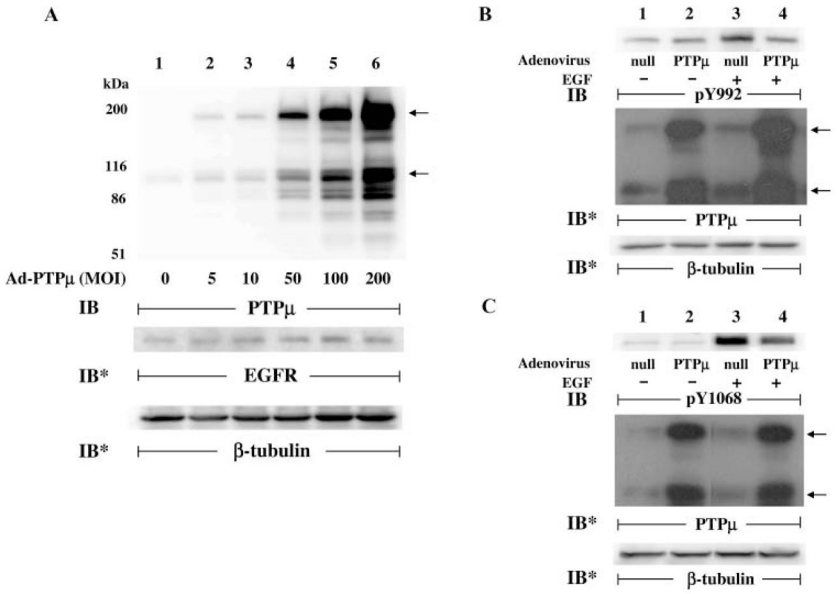

FIGURE 4.

PTPμ overexpression decreases EGF-stimulated EGFR tyrosine phosphorylation. (**A**) A549 cells were transiently infected with increasing MOIs of Ad-PTPμ or incubated with medium alone. At 48 hours, cells were lysed and the lysates processed for PTPμ immunoblotting. Blots were stripped and reprobed for total EGFR and β-tubulin. Molecular weight in kDa is indicated on the left. (**B** and **C**) A549 cells were transiently infected with Ad-PTPμ or Ad-null (MOI = 100). At 24 hours, the cells were serum starved for an additional 24 hours, after which they were treated for 10 minutes with EGF (100 ng/mL) (lanes 3 and 4) or medium alone (lanes 1 and 2). Cells were lysed and the lysates processed for phospho-EGFR immunoblotting with antibodies to either PY992 (**B**) or PY1068 (**C**). To control for both PTPμ expression and protein loading and transfer, blots were stripped and reprobed for PTPμ and β-tubulin. IB = immunoblot; IB* = immunoblot after stripping. Arrows on right indicate full-length (~200-kDa) and proteolytically cleaved (~100-kDa) PTPμ immunoreactive bands. Each blot is representative of ≥2 independent experiments.

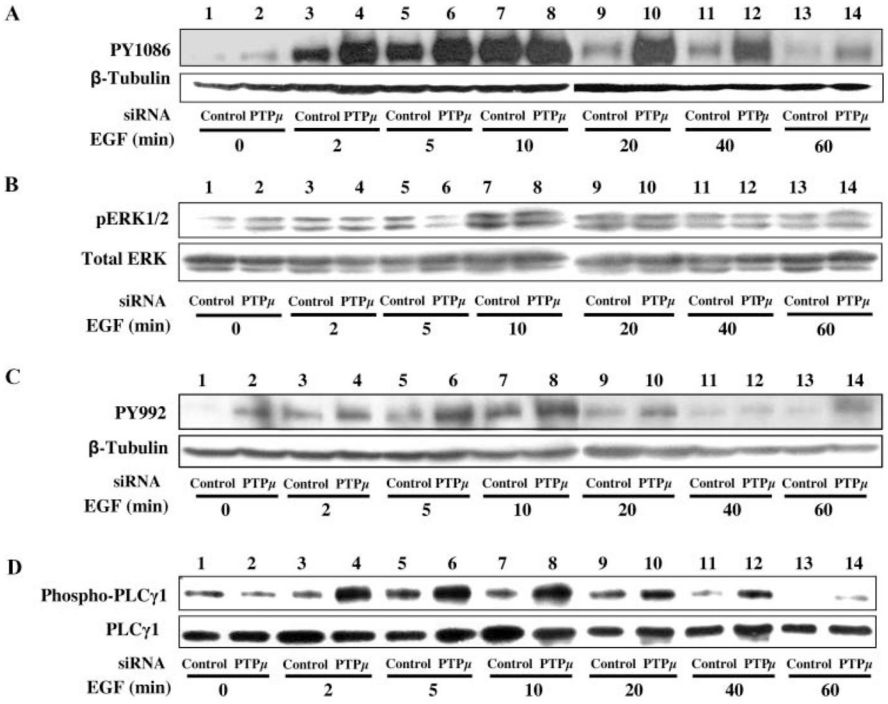

FIGURE 5.

Reduced PTPμ expression increases EGFR phosphorylation on Y992 and Y1086 and activates PLCγ_1 without altering ERK1/2 phosphorylation. A549 cells were transfected with control or PTPμ-targeting siRNA duplexes, after which they were serum starved for 24 hours prior to treatment for increasing times with EGF (100 ng/mL) or medium alone. (**A**) Cells were lysed and lysates processed for phospho-EGFR (Y1086) immunoblotting. (**B**) The same samples were immunoblotted for phosphoERK1/2. To control for loading, blots were stripped and reprobed for total ERK. (**C**) Cells were lysed and lysates processed for phospho-EGFR (Y992) immunoblotting. (**D**) Cell were lysed and lysates processed for phospho-PLCγ_1 immunoblotting. To control for loading, blots were stripped and reprobed for total PLCγ_1. In **A** and **C**, to control for loading, blots were stripped and reprobed for β-tubulin. These blots are representative of ≥3 experiments.

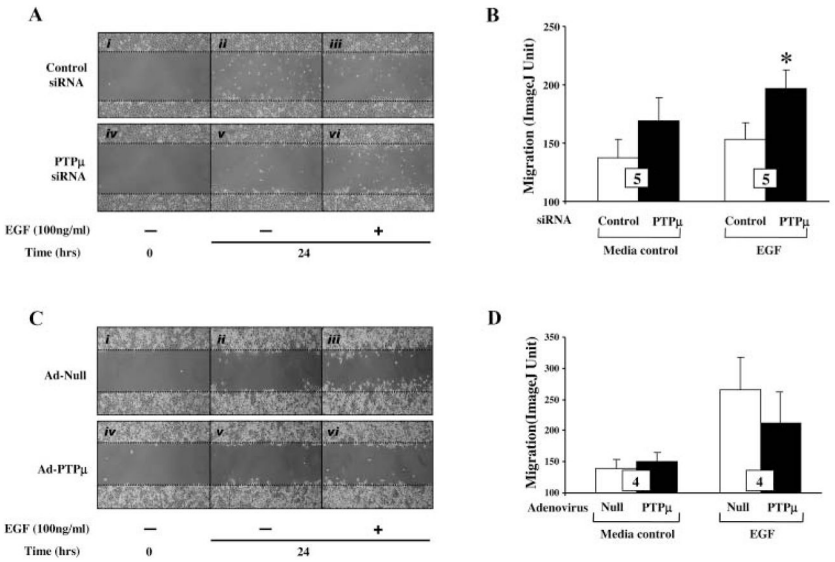

FIGURE 6.

PTPμ counterregulates A549 cell migration in a wounding assay. A549 cells were transfected with PTPμ-targeting or control siRNAs, or transiently infected with Ad-PTPμ or Ad-null (MOI = 100), and cultured to confluence in the wells of 6-well plates. After 48 hours, serum-starved monolayers were wounded with a sterile pipette tip, washed, and cultured for 24 hours in the presence and absence of EGF (100 ng/mL). (**A** and **C**) At 0 and 24 hours, triplicate images of each monolayer were captured through a microscope (100×), and migration into the wound at 24 hours compared to that seen in the same wounded monolayer at 0 hour. Dotted lines indicate wound boundaries at 0 hour. (**B** and **D**) Mean (± SE) migration of cells into the wound was measured in each well in triplicate. *n*, the number of independent experiments, is indicated. *Significantly increased compared to the control siRNA-transfected cells at $P < .05$.

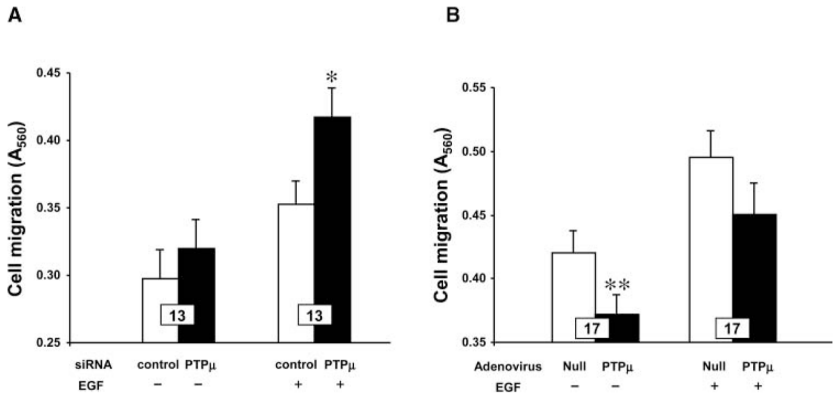

FIGURE 7.

PTPμ counterregulates A549 cell migration in a chemotaxis assay. (**A**) A549 cells transfected with either PTPμ-targeting or control siRNAs were placed in the upper compartments of chemotaxis chambers at 2×10^5 cells in 0.8 mL/chamber. The lower compartments contained EGF 1 ng/mL and 0.1% FBS. (**B**) A549 cells were infected with either Ad-PTPμ or Ad-null at MOI of 100 and added to the upper compartments of chemotaxis chambers (2×10^5 cells/chamber) in which each lower compartment contained EGF 10 ng/mL and 0.1% FBS. After 5 hours, filters were removed, fixed, stained with crystal violet, washed, and the top surface scraped free of cells. The crystal violet was extracted from each filter and A_{560nm} measured. Each vertical bar represents mean (± SE) cell migration. The number of independent experiments are indicated within the bars. *Significantly increased compared to the control siRNA-transfected cells at $P < .05$. **Significantly decreased compared to the Ad-null infected cells at $P < .05$.

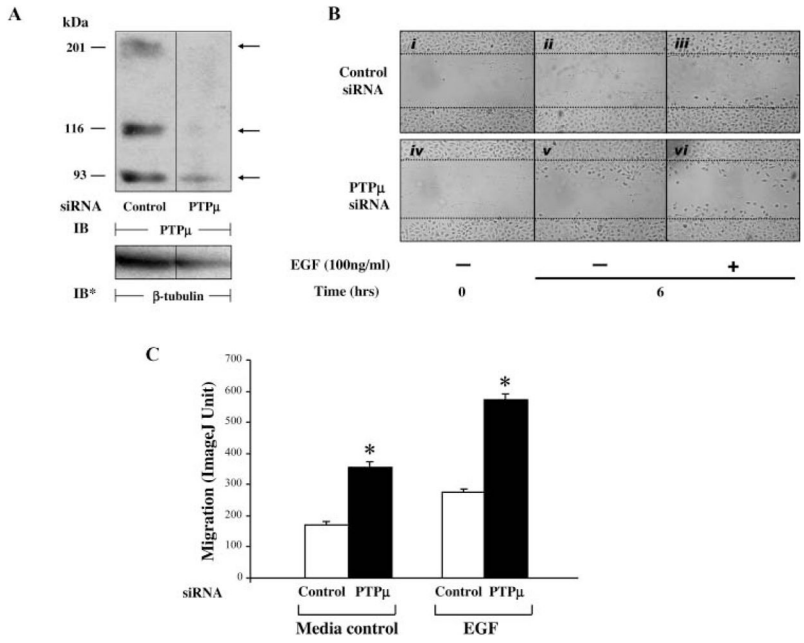

FIGURE 8.

PTPμ counterregulates SAEC migration in a wounding assay. (**A**) Confluent primary human small airway epithelial cells (SAECs) were transfected with control (lane 1) or PTPμ-targeting (lane 2) siRNAs, lysed, and the lysates processed for PTPμ immunoblotting. To control for protein loading and transfer, blots were stripped and reprobed for β-tubulin. IB = immunoblot; IB* = immunoblot after stripping. (**B** and **C**) In other studies, SAECs transfected with PTPμ-targeting or control siRNAs were cultured to confluence in the wells of 6-well plates ($n = 6$). After 48 hours, serum-starved monolayers were wounded with a sterile pipette tip, washed, and cultured for 6 hours in the presence or absence of EGF (100 ng/mL). (**B**) At 0 and 6 hours, triplicate images of each monolayer were captured through a microscope and migration into the wound at 6 hours was compared to that seen in the same wounded monolayer at 0 hour. Dotted lines indicate wound boundaries at 0 hour (100×). (**C**) Mean (± SE) migration of cells into the wound was measured in each well in triplicate. *Significantly increased compared to the control siRNA-transfected cells at $P < .05$.